

Melting the Fullerenes: A Molecular Dynamics Study

Seong Gon Kim and David Tománek

*Department of Physics and Astronomy and Center for Fundamental Materials Research,
Michigan State University, East Lansing, Michigan 48824-1116*

(Received 29 November 1993)

We report a molecular dynamics simulation of melting and evaporation of the carbon fullerenes C_{20} , C_{60} , and C_{240} . Several phases, among them a previously unknown “pretzel” phase with a three-dimensional structure of multiply connected carbon rings, can be identified above the high initial melting temperature $T \approx 4000$ K. At $T \gtrsim 10^4$ K, a complete conversion of compact fullerenes to carbon chain fragments is driven by entropy.

PACS numbers: 61.46.+w, 36.40.+d, 82.30.Lp

Carbon fullerenes, such as C_{60} [1], are intriguing molecules with a hollow soccer ball structure and a large range of interesting properties [2]. Because of the high structural stability of these systems [3], almost no information is available about their equilibrium phases at temperatures close to and exceeding the melting point of graphite. We expect the phase diagram of these strongly correlated structures to be very interesting and to consist of several well identifiable “molten” phases.

A second reason to study the high-temperature behavior of fullerenes is related to their formation. While bulk quantities of fullerenes can now be routinely synthesized in a carbon arc [4], the microscopic mechanism of their aggregation from gas phase is still the subject of significant controversy [5–9]. We believe that a detailed study of the annealing process may shed new light on this controversy, since intermediate structures, which occur during thermal quenching in the rare gas atmosphere, may also be observed while heating up these structures to high temperatures.

A third motivating reason for this study are recent collision experiments which indicate that fullerene molecules are extremely resilient and only fragment at energies exceeding ≈ 200 eV [10]. Since in the collision process the kinetic energy is transferred into internal degrees of freedom as “heat,” additional information about the intermediate structures of colliding fullerenes could be obtained by investigating those of the superheated molecules.

In an attempt to elucidate the above three problem areas, we performed a detailed molecular dynamics (MD) study of the melting and evaporation process of three prototype fullerenes, namely, C_{20} , C_{60} , and C_{240} . In our simulation, we investigated the response of a canonical ensemble of fullerenes to gradually increasing heat bath temperatures using Nosé-Hoover molecular dynamics [11,12], complementing recent microcanonical ensemble simulations on C_{60} and C_{70} [13]. Of course, the quality of simulation results depends primarily on the adequacy of the total energy formalism applied to the fullerenes. Since our simulation also addresses the fragmentation under extreme conditions, the formalism used must accurately describe the relative stability of

fullerenes with a graphitic structure and their fragments, mostly short carbon chains. The corresponding transition from sp^2 to sp bonding can only be reliably described by a Hamiltonian which explicitly addresses the hybridization between C $2s$ and C $2p$ orbitals. A precise evaluation of interatomic forces is required to obtain the correct long-time behavior of the system. On the other hand, the long simulation runs necessary to equilibrate the small systems during the annealing process, and the large ensemble averages needed for a good statistics, virtually exclude *ab initio* techniques as viable candidates for the calculation of atomic forces.

For this reason, we base our force calculation on a linear combination of atomic orbitals formalism which conveniently parametrizes *ab initio* local density functional results for structures as different as C_2 , carbon chains, graphite, and diamond [14]. We use an adaptation of this formalism to very large systems, which is based on the fact that forces depend most strongly on the local atomic environment and which has been implemented using the recursion technique [15]. The force calculation can be performed analytically to a large degree. This not only speeds up the computations significantly, but also provides an excellent energy conservation $\Delta E/E \lesssim 10^{-10}$ between time steps in microcanonical ensembles, and a linear scaling of the computer time with the system size. Most important, forces on distant atoms can be efficiently calculated on separate processors of a massively parallel computer.

In our MD simulations, we use the leapfrog technique to integrate the equations of motion over time steps $\Delta t = 5 \times 10^{-16}$ s. We begin each MD run by equilibrating the particular fullerene for 300 time steps at a temperature $T_i = 1000$ K, after the directions of the initial atomic velocities have been randomized. We increase the temperature of the heat bath in steps of $\Delta T = 400$ K from T_i to the final temperature $T_f = 10\,000$ K, and let the fullerenes equilibrate for 800 time steps at each new temperature. Each simulation run consists of 20 000 time steps and takes several hours of CPU time on a high-speed single-processor workstation. Statistical (time-averaged) data for the structure and energetics are col-

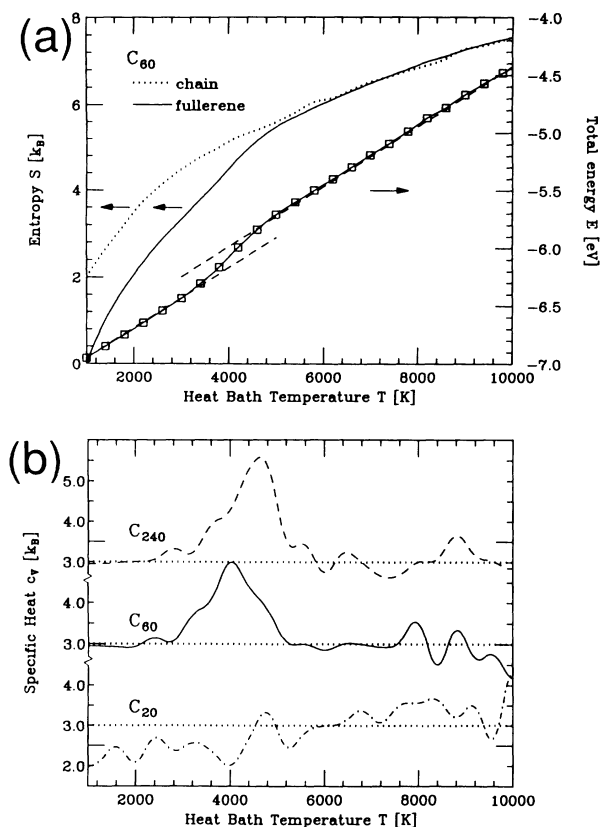


FIG. 1. (a) Temperature dependence of the total energy E and the entropy S per atom for the C_{60} fullerene (solid line) and the metastable C_{60} chain (dotted line). The data points in the $E(T)$ curve for the fullerene mark the discrete steps of the heat bath temperature used, and the dashed lines with a slope of $3k_B$ are guides to the eye. (b) Specific heat $c_V(T)$ per atom of icosahedral fullerenes C_{240} (dashed line), C_{60} (solid line), and C_{20} (dash-dotted line), in the temperature range $T < 10000$ K, in units of k_B . The ordinate is displaced vertically between successive plots for clarity; the classical value $c_V = 3k_B$ is indicated by the dotted lines.

lected after the system has adjusted to the new temperature, which is typically after 400 time steps following a temperature increase. A separate ensemble averaging at each temperature is necessary since ergodicity is not guaranteed especially in very small systems. We perform ensemble averaging over 50 complete runs with different initial states of C_{20} , 50 runs for C_{60} , and 15 runs for C_{240} . This reflects the decreasing fluctuations of thermodynamic quantities with increasing system size.

In Fig. 1(a), we present results for the temperature dependence of the total energy E and the entropy S per atom for the C_{60} molecule. We observe a steady increase of E and S with increasing temperature, with a well-formed step at $T \approx 4000$ K indicative of a "phase transition." To get a better understanding of the structural transformations in this and other fullerenes, we investigated the specific heat not only of the C_{60} , but also the

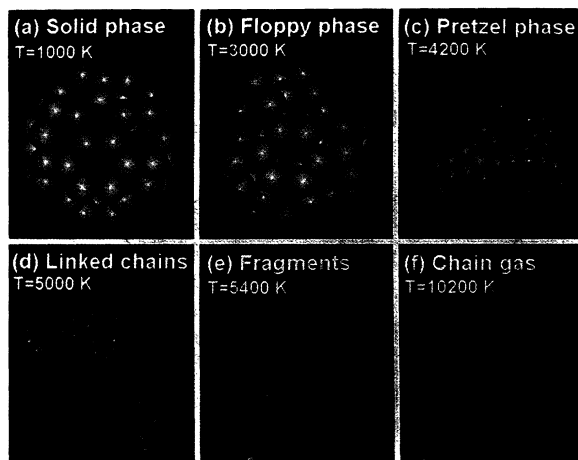


FIG. 2. "Snap shots" illustrating the geometry of a C_{60} cluster at temperatures corresponding to the different "phases" discussed in the text.

C_{20} and the C_{240} molecules. The calculated temperature dependence of the specific heat per atom of these systems, obtained from $c_V = dE/dT$, is shown in Fig. 1(b). In the temperature range addressed in this study, we found significant deviations from the classical value $c_V = 3k_B$ to occur only for $T \gtrsim 2000$ K. We found all features in the rich structured $c_V(T)$ to be reproducible from run to run up to a temperature of $T \approx 6000$ K. Individual peaks in c_V reflect the latent heat of transition between different "phases." As we discuss in the following, these phases can be characterized by their topology and atomic binding energy distributions. In contrast to phase transitions in solids, the analogous transitions in fullerenes are not sharp owing to the finite size of these systems.

Because of the similarity of the $c_V(T)$ results for the different fullerenes, we concentrate in the following on the C_{60} molecule. In order to identify the characteristics of its individual phases, we show in Fig. 2 characteristic "snap shots" of the C_{60} structure, and in Fig. 3 the binding energy distribution of individual atoms in the C_{60} at selected heat bath temperatures. We find the binding energy distribution to provide a better signature of the different phases than topological quantities (such as coordination numbers) which depend on the definition of cutoff distances.

In the *solid phase*, occurring at $T \lesssim 2400$ K and depicted in Fig. 2(a), the C_{60} is intact. As shown in Fig. 3(a), the binding energy of all atoms is approximately the same, but decreases gradually with increasing temperature due to thermal expansion.

A peak in the $c_V(T)$ curve at $T \approx 2400$ K indicates the gradual onset of the *floppy phase*, depicted in Fig. 2(b). While the system is topologically intact in this phase, as documented by a narrow bond length distribution, we observe the bond angle distribution to spread out, resulting

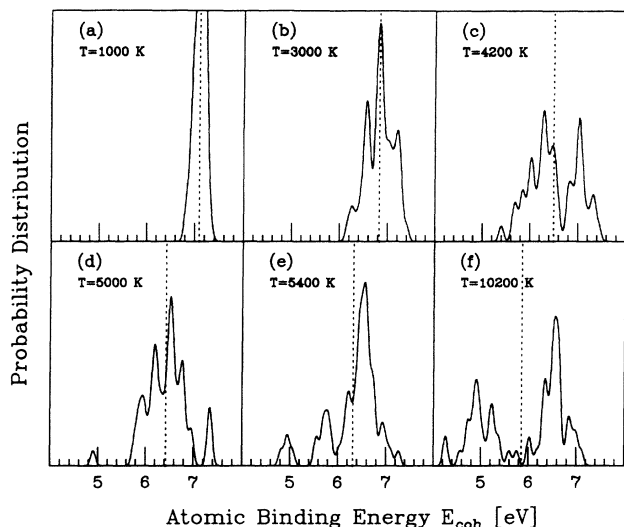


FIG. 3. Atomic binding energy distribution in a C_{60} cluster at temperatures characteristic of the different “phases” discussed in the text and in Fig. 2. For each structure, the average binding energy is given by the dotted line.

in a significantly broadened binding energy distribution [Fig. 3(b)]. Assisted by local shear motion, carbon pentagons and hexagons tilt easily with respect to the surface normal especially in large fullerenes with flat faces. In C_{60} , this floppy motion creates a bimodal distribution of carbon sites which are either closer to or further away from the optimum graphitic bonding geometry than the average structure. We found that the local shear motion leads to substantial cluster shape deformations.

Above $T \approx 4000$ K, we observe a dramatic transition to the *pretzel phase*, consisting of interconnected carbon rings and depicted in Fig. 2(c). A similar, yet not as complex structure has recently been proposed as a high temperature phase of C_n clusters based on diffusion data [8,9]. In our calculation, we find this structure to be initiated by the rupture of a single bond connecting a pentagon to a hexagon, which creates a large opening at the surface. As shown in Fig. 1(a), the transition from a (two-dimensional) fullerene to a (one-dimensional) linked chain structure is clearly reflected in a sharp increase of the entropy towards a value characteristic of a (metastable) C_{60} chain. The energetically less favorable *sp* bonding of a growing number of twofold coordinated atoms in the “pretzel” phase is reflected in the broadening of the binding energy distribution especially towards lower values. This is shown in Fig. 3(c) for a fully developed pretzel at $T = 4200$ K. The specific heat data of Fig. 1(b) suggest that the critical temperature shifts upward with increasing fullerene size.

Closed carbon chains of the C_{60} pretzel open up at $T \gtrsim 5000$ K, as shown in Fig. 2(d). The number of structural constraints in this *linked chain* phase decreases, allowing individual atoms to relax. This leads to a smaller number

of inequivalent sites and more pronounced peaks in the binding energy distribution, depicted in Fig. 3(d).

Starting at $T \approx 6000$ K, we observe fragmentation of all fullerenes which we studied. Typical fragments, such as those shown in Fig. 2(e) for $T = 5400$ K, have pretzel and “linked chain” structures discussed above. Above this temperature, the thermodynamics of the system is that of fullerene fragments; strong run-to-run fluctuations are caused by the differences in the specific heat of the individual fragments. While the binding energy range is similar to that in the linked chain phase, the distribution is smoother at this higher temperature, as shown in Fig. 3(e). Finally, at temperatures close to $T \approx 10000$ K, a conversion to a chain gas is completed, as illustrated in Fig. 2(f).

The temperature scale relevant to structural transitions in fullerenes can be linked to well established thermodynamic data for graphite [16]. We find the “floppy phase” of fullerenes to occur at temperatures close to the melting point of graphite, $T_{mp} = 3823$ K [16]. On the other hand, the calculated fragmentation temperature $T \approx 5400$ K lies close to the observed boiling point of graphite, $T_{bp} = 5100$ K [16].

In order to understand the rich “phase diagram” of fullerenes, we have to investigate the free energy F as a function of temperature. It is intuitively clear that the more “floppy” chain structures have a larger entropy and hence should be preferred over the more compact fullerene structures at sufficiently high temperatures. As mentioned above, we have determined the entropy $S(T)$ per atom from MD simulation runs of C_{60} fullerenes and metastable C_{60} chains. Our results, shown in Fig. 1(a), indicate that the entropy values are equal at very high temperatures where also the fullerenes have converted to linear structures. Prior to the conversion, we find for the entropy difference $S(C_{60} - \text{chain}) - S(C_{60} - \text{fullerene}) \approx 2k_B$. This allows us immediately to estimate the conversion temperature from fullerenes to chains from low temperature data, using $F(\text{chain}) - F(\text{fullerene}) = [E(\text{chain}) - E(\text{fullerene})] - T_c[S(\text{chain}) - S(\text{fullerene})] = 0$, which yields $T_c = \Delta E / \Delta S$. Using $\Delta E = E(\text{chain}) - E(\text{fullerene}) \approx 1$ eV [14] and assuming that the values for ΔE and $\Delta S = S(\text{chain}) - S(\text{fullerene})$ are nearly temperature independent, we obtain $T_c \approx 5800$ K for the fullerene-to-chain conversion, in rough agreement with our simulation results.

It is interesting to note that the open fullerene phases, which were identified in our simulation, also occur during energetic collisions between fullerenes. In particular, the final state of a C_{60} cluster undergoing an inelastic collision with a C_{240} cluster at 300 eV center-of-mass kinetic energy heats up during the collision process to temperatures close to 5000 K and shows a final structure similar to that presented in Fig. 2(d) [17].

Our results shed new light also on the formation process of fullerenes from the gas phase. While time reversal of the evaporation process studied here would pro-

vide *one possible* aggregation path, the general formation mechanism is clearly more complex. We expect that many structures which occur during the fragmentation also reoccur during the aggregation. Of course, most of the “random” aggregation paths will not lead immediately to a closed fullerene, yet are likely to contain stable structural elements such as chains and rings. Once such a linked chain or “fragmented pretzel” structure is formed, the aggregation dynamics will be governed by many unsuccessful attempts to reversibly “roll up” the chains to a fullerene, followed by one successful attempt to create an inert structure. This picture agrees with the fullerene formation mechanism suggested in Ref. [9] and the isotope scrambling results of Ref. [6] suggesting that gas phase assembly of fullerenes starts from atoms and very small carbon clusters.

In summary, we presented molecular dynamics simulation results of the melting and evaporation of the carbon fullerenes C_{20} , C_{60} , and C_{240} . Among others, we found a most dramatic transition to a pretzel phase to occur at a high temperature of $T \gtrsim 4000$ K. The temperature where fullerenes disintegrate into carbon chains was explained using quantitative results for the entropy.

The authors would like to thank George Bertsch for useful discussions, Weiqing Zhong for codeveloping and coding the many-body force functional, and Richard Enbody for his assistance in the parallel implementation of the codes. This work was supported by the National Science Foundation under Grant No. PHY-8920927.

[1] H.W. Kroto, J.R. Heath, S.C. O'Brien, R.F. Curl, and

- R.E. Smalley, *Nature (London)* **318**, 162 (1985).
 [2] Properties of fullerenes, their derivatives in the gas and in the bulk phase are reviewed in a series of articles in *Buckminsterfullerenes*, edited by W.E. Billups and M.A. Ciufolini (VCH Publishers, New York, 1993).
 [3] Robert F. Curl and Richard E. Smalley, *Science* **242**, 1017 (1988).
 [4] W. Krätschmer, L.D. Lamb, K. Fostiropoulos, and D.R. Huffman, *Nature (London)* **347**, 354 (1990).
 [5] T. Wakabayashi and Y. Achiba, *Chem. Phys. Lett.* **190**, 465 (1992); **201**, 470 (1993).
 [6] T.W. Ebbesen, J. Tabuchi, and K. Tanigaki, *Chem. Phys. Lett.* **191**, 336 (1992).
 [7] R. Kerner, K.A. Penson, and K.H. Bennemann, *Europhys. Lett.* **19**, 363 (1992).
 [8] G. von Helden, N.G. Gotts, and M.T. Bowers, *Nature (London)* **363**, 60 (1993).
 [9] Joanna M. Hunter, James L. Fye, Eric J. Roskamp, and Martin F. Jarrold, *J. Phys. Chem.* **98**, 1810 (1994).
 [10] E.E.B. Campbell, V. Schyja, R. Ehlich, and I.V. Hertel, *Phys. Rev. Lett.* **70**, 263 (1993); H.G. Busmann, T. Lill, B. Reif, and I.V. Hertel, *Surf. Sci.* **272**, 146 (1992).
 [11] W.G. Hoover, *Phys. Rev. A* **31**, 1695 (1985); S. Nosé, *Mol. Phys.* **52**, 255 (1984).
 [12] M.P. Allen and D.J. Tildesley, *Computer Simulation of Liquids* (Oxford, New York, 1990).
 [13] Eunja Kim, Young Hee Lee, and Jae Young Lee, *Phys. Rev. B* **48**, 18 230 (1993).
 [14] David Tománek and Michael A. Schluter, *Phys. Rev. Lett.* **67**, 2331 (1991).
 [15] W. Zhong, D. Tománek, and George F. Bertsch, *Solid State Commun.* **86**, 607 (1993).
 [16] *CRC Handbook of Chemistry and Physics* (CRC Press, Boca Raton, FL, 1990), 62nd ed., p. B-10.
 [17] S. G. Kim, W. Zhong, and D. Tománek (to be published).

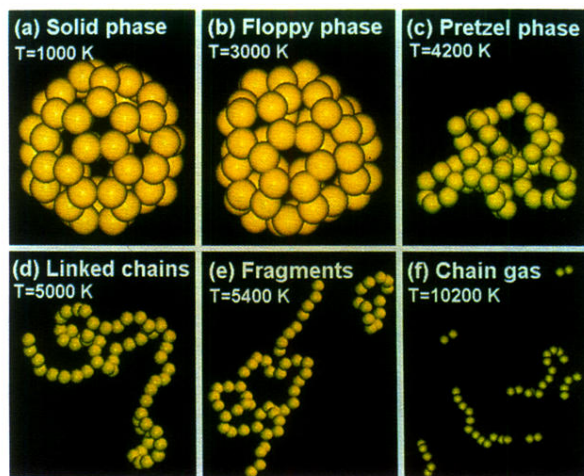


FIG. 2. “Snap shots” illustrating the geometry of a C_{60} cluster at temperatures corresponding to the different “phases” discussed in the text.